Energetically consistent rotated diffusion and lateral stirring surfaces in the ocean

Tailleux, R. ORCID: https://orcid.org/0000-0001-8998-9107
(2026) Energetically consistent rotated diffusion and lateral stirring surfaces in the ocean. Ocean Modelling, 202. 102722. ISSN 1463-5011 doi: 10.1016/j.ocemod.2026.102722
Available at https://centaur.reading.ac.uk/128864/

Ocean Modelling 202 (2026) 102722

Contents lists available at ScienceDirect

Ocean Modelling

journal homepage: www.elsevier.com/locate/ocemod

Energetically consistent rotated diffusion and lateral stirring surfaces in the ocean

Rémi Tailleux

Department of Meteorology, University of Reading, Whiteknights road, Earley Gate, Reading, RG6 6ET, United Kingdom

ARTICLE INFO

Keywords:
Available potential energy
Rotated diffusion
Isopycnal surfaces
Lateral stirring
Energetic consistency
Spurious mixing

ABSTRACT

The definition of isopycnal surfaces in the ocean has long remained ambiguous, complicating the parameterisation of subgridscale mixing in ocean models and rigorous development of isopycnic-coordinate frameworks. Here we show that balancing sources and sinks of subgridscale turbulent available potential energy (TAPE) constrains isopycnal surfaces to align with the Lorenz reference density (LRD) surfaces that define the reference state in APE theory. Building on this, comparisons in (S,θ) space confirm that LRD surfaces form the underlying physical basis for empirical approximately neutral surfaces (γ^n and Ω), except in colder waters. In our theory, deviations from neutrality are the signatures of thermobaric forces rather than 'errors'. Consequently, constructing rotated (Redi) diffusion tensors using neutral directions is unphysical, as it introduces spurious diapycnal mixing via the Veronis effect — particularly significant in the Southern Ocean. This highlights APE theory as a fundamental framework for developing energetically consistent ocean models and parameterisations, offering a pathway to reduce or eliminate artificial diapycnal mixing in ocean general circulation models (OGCMs).

1. Introduction

Accurate representation of small-scale mixing processes is critical for simulating ocean circulation, heat and carbon uptake, and climate variability. Climatically important features such as meridional heat transport and the Atlantic Meridional Overturning Circulation (AMOC) are sensitive to irreversible tracer and momentum mixing at scales unresolved by ocean general circulation models (OGCMs). Modelled behaviour is strongly influenced both by physical parameterisations and by unavoidable numerical mixing introduced through the discretisation of advection and other processes (Griffies et al., 2000).

In practice, OGCMs employ parameterisations with skew-symmetric and symmetric components to represent mesoscale eddy effects and subgrid-scale mixing of heat and salt. The skew part acts as an eddy-induced advection (Gent and McWilliams, 1990; Gent et al., 1995; Griffies, 1998), while the symmetric part mixes tracers along designated "lateral" directions (traditionally called isopycnal or isoneutral) and vertically (or diapycnally) across them (Solomon, 1971; Redi, 1982; McDougall and Church, 1986; Griffies et al., 1998; Lemarié et al., 2012; McDougall et al., 2014). Despite decades of progress, fundamental uncertainty remains about what these lateral mixing directions should be and how to ensure that such choices are energetically consistent.

A growing consensus is that energetics should constrain parameterisations. Energy is continually exchanged between resolved and subgridscale reservoirs, and each exchange must respect the fundamental budgets of kinetic energy (KE), available potential energy (APE), and background potential energy (BPE), alongside their interconversions. In turbulent stratified fluids, viscous stresses dissipate KE at a rate ε_K, while molecular diffusion dissipates APE into BPE at a rate ε_p, thereby setting the diapycnal diffusivity K_v (Oakey, 1982; Gargett and Holloway, 1984; Winters et al., 1995; Lindborg and Brethouwer, 2008). This recognition motivates "energetically consistent" parameterisations, in which subgrid tendencies are evaluated and constrained via their implied energy pathways (Marshall et al., 2012; Eden et al., 2014; Eden, 2015, 2016; Mak et al., 2018; Torres et al., 2023).

In simple fluids such as the dry atmosphere or freshwater, lateral stirring can be idealised as adiabatic and aligned with isentropic surfaces; such exchanges leave the stratification and total potential energy (PE) unchanged. In seawater, however, this is precluded by the thermobaric nonlinearity of the equation of state: cold parcels are more compressible than warm ones, so adiabatic and isohaline exchanges inevitably alter both internal energy (IE) and gravitational potential energy (GPE). Stirring along "neutral directions" — classically defined by the neutral vector $\mathbf{n} = \alpha\nabla\theta - \beta\nabla S$ — appears to leave the PE unaffected only because changes in APE are compensated by opposite changes in

E-mail address: r.g.j.tailleux@reading.ac.uk.

https://doi.org/10.1016/j.ocemod.2026.102722
Received 8 October 2025; Received in revised form 18 February 2026; Accepted 2 March 2026
Available online 7 March 2026

BPE, where α and β are the thermal expansion and haline contraction coefficients, respectively. Within APE theory, these compensating transfers are precisely the energetic signature of diapycnal mixing. This perspective reveals that isoneutral mixing can project spuriously onto diapycnal mixing via the long-recognised Veronis effect (Veronis, 1975).

So far, most attention has focused on the turbulent kinetic energy (TKE) budget as the main tool for constraining parameterisations. Here we argue, instead, that it is the turbulent APE (TAPE) budget that provides the fundamental constraint on both vertical mixing rates and the appropriate definition of lateral stirring surfaces in seawater. Recent theory shows that, under statistical stationarity and homogeneity, the eddy APE production — fed by conversions from eddy KE and mean APE — must balance the turbulent APE dissipation rate ε_p, determining the diapycnal diffusivity $K_v \approx \varepsilon_p/\overline{N}^2$ (Tailleux and Roullet, 2025). The key new insight is that eddy APE production depends sensitively on the choice of lateral stirring directions used by the rotated diffusion tensor. We show that only one choice yields energetic consistency: the directions tangent to Lorenz reference density (LRD) surfaces, i.e. the isosurfaces of the minimum-PE Lorenz state central to APE theory. With this choice, eddy APE production becomes independent of the large isopycnal diffusivity K_i and is controlled solely by physical diapycnal processes, thereby eliminating the Veronis effect. Conversely, constructing rotated diffusion in terms of the neutral directions employed in most OGCMs induces a fictitious diapycnal diffusivity proportional to K_i, potentially significant in the Southern Ocean where departures from the Lorenz reference state are large.

This APE-based viewpoint reframes the long-standing debate about density coordinates and isopycnal surfaces in oceanography. Classical efforts have centred on the construction of neutral surfaces (McDougall, 1987a). However, the neutral vector $\mathbf{n}$ is non-integrable, so exact neutral surfaces do not exist. In practice, approximate neutrality is enforced by minimising departures from neutrality, typically treated as an "error", leading to the construction of empirical approximately neutral surfaces (ANS) — including patched potential density (Lynn and Reid, 1968), neutral density γ^n (Jackett and McDougall, 1997), and Ω-surfaces (Klocker et al., 2009; Stanley et al., 2021). Experience shows that while neutrality can be accurately enforced in much of the ocean interior, this is more difficult in regions such as the Southern Ocean where thermobaric effects appear to be unavoidably large. Yet the physical quantity that ANS are meant to represent has remained ambiguous, preventing any objective evaluation of their success. Our analysis resolves that ambiguity by suggesting that LRD surfaces are the physical object that ANS actually seek to emulate. We further propose that departures from neutrality should not be regarded as "errors" to be eliminated, but as the manifestation of thermobaric forces — an intrinsic physical effect central to the energetics of lateral stirring in seawater.

The remainder of the paper is organised as follows. Section 2 recalls the main results of Tailleux and Roullet (2025), establishing the link between parameterised and actual mixing via an exact mean/eddy APE decomposition. This approach recovers standard relations between ε_p and diapycnal diffusivity while clarifying the underlying assumptions. The key results are: (i) mixing parameterisations of heat and salt control not only the energy transfers between resolved and unresolved reservoirs, but also those between unresolved kinetic energy and unresolved available potential energy, a point that is often overlooked; and (ii) the budget of unresolved/eddy APE fundamentally constrains the turbulent diapycnal flux.

Section 3 extends this analysis to realistic seawater and derives an energetics-based criterion that selects LRD surfaces as the correct stirring directions for rotated diffusion. Prior to this, we contrast the properties of LRD surfaces with empirical ANS in (S,θ) space, empirically establishing the former as the physically well-defined surfaces that ANS seek to approximate, particularly outside the Southern Ocean. These results imply that LRD surfaces should form the basis for specifying lateral stirring directions in rotated diffusion tensors, and that using neutral directions necessarily induces spurious diapycnal mixing, thereby providing a rigorous definition of the Veronis effect. They also clarify the link between turbulent diapycnal/vertical diffusivities used in models and diffusivities inferred from observations.

Section 4 estimates the magnitude of spurious diapycnal mixing associated with the use of neutral rotated diffusion and demonstrates that it is significant in the Southern Ocean. We suggest that this effect may explain the unexpected sensitivity of ocean stratification and circulation to isoneutral mixing reported by Forget et al. (2015) and Chouksey et al. (2022). This section also discusses the implications for developing APE-based diagnostics to evaluate spurious diapycnal mixing in numerical ocean models. In particular, because turbulent diapycnal mixing relates to the dissipation of subgrid-scale APE, diagnosing it in a numerical ocean model requires understanding how the sinks and sources of resolved APE relate to the sinks and sources of unresolved APE. Finally, Section 5 summarises the main findings and outlines priorities for implementing APE diagnostics and extending the theory to non-resting reference states where the ocean state departs significantly from the Lorenz reference state.

2. Linking parameterised energy transfers to dissipative processes

In the modern view of ocean energetics, mechanical and thermodynamic energy input is ultimately dissipated at small scales through two main pathways: (i) viscous processes, at the turbulent KE dissipation rate ε_K^t, and (ii) molecular diffusion, at the turbulent APE dissipation rate ε_p^t. These physical dissipation rates a priori differ from the 'resolved' dissipation rates D_K and D_A associated with the energy transfers between resolved KE and APE and their subgridscale counterparts induced by subgrid parameterisations of momentum, heat, and salt. The central aim of *energetically consistent* modelling — pioneered by Eden et al. (2014), Eden (2015, 2016) — is to clarify how such parameterised energy transfers relate to their true molecular counterparts. Eden and co-workers decomposed potential energy into dynamic and potential enthalpy following Young (2010) and Nycander (2010). However, because turbulent diapycnal mixing represents a conversion between APE and BPE (Winters et al., 1995; Tailleux, 2009), it is more natural to retain Lorenz's original partition into available and background potential energy (Lorenz, 1955).

Unlike most previous APE-based studies, our approach builds on *local* APE theory to avoid the unphysical features of the global APE framework (Scotti and White, 2014; Zemskova et al., 2015; Tailleux, 2018, 2024; Tailleux and Roullet, 2025). Local APE theory allows APE — as well as mean and eddy reservoirs — to be defined for individual fluid parcels, analogous to KE, rather than only as volume integrals. Throughout this paper, we interpret 'mean' and 'eddy' as 'resolved' and 'unresolved', respectively. This simple two-way split — resolved vs. unresolved — is sufficient for our purposes, even if less elaborate than the multi-scale partitions into large-scale flow, mesoscale eddies, internal gravity waves, and turbulence proposed by Eden (2015).

Fig. 1 schematically illustrates the impact of the turbulent density flux $\overline{\rho'\mathbf{v}'}$ on the energy transfers between resolved and unresolved KE and APE reservoirs, as derived by Tailleux and Roullet (2025) for a simple Boussinesq fluid with a linear equation of state (see below for more details). This schematic highlights that the turbulent density flux controls not only the transfers between resolved and unresolved reservoirs (here, between resolved and unresolved APE), but also transfers between unresolved reservoirs (between unresolved KE and unresolved APE). Fig. 2 illustrates the corresponding implications for numerical ocean general circulation models. The resolved reservoirs (E_k^m, E_a^m) exchange energy with their unresolved counterparts (E_k^t, E_a^t) through parameterisations: (i) momentum mixing (MM), (ii) mesoscale eddies (GM), and (iii) rotated diffusion (RD). In steady state, MM and GM transfer energy into unresolved KE, which must be balanced by ε_K^t and

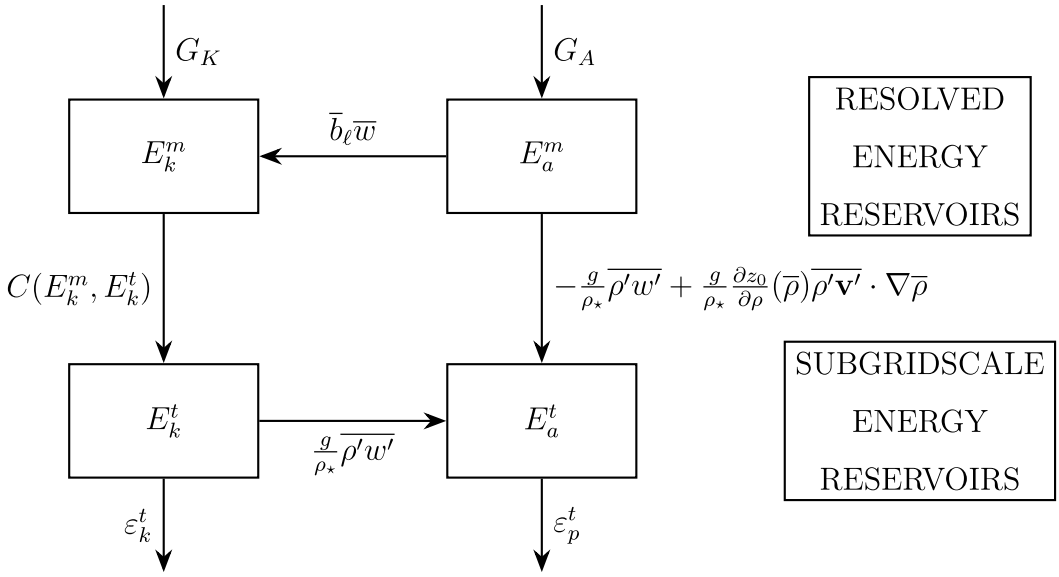

Fig. 1. Schematics of theoretical energy transfers between resolved and unresolved reservoirs predicted by the exact mean/eddy decomposition of Tailleux and Roullet (2025). This theory highlights the fact that the turbulent density flux $\overline{\rho' \mathbf{v}'}$ not only controls energy transfers between resolved and unresolved energy reservoirs (E_a^m and E_a^t), but also between unresolved energy reservoirs (E_k^t and E_a^t).

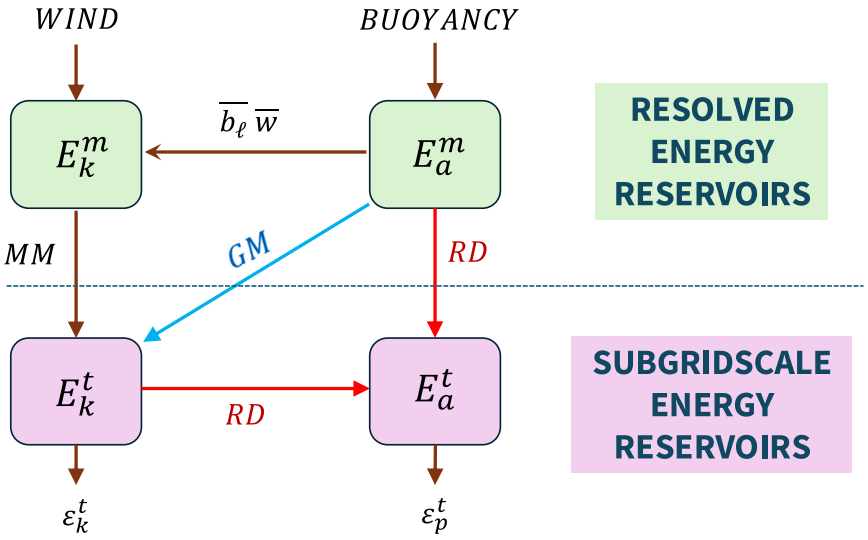

Fig. 2. Idealised energy diagram showing the conversions between resolved and subgrid-scale energy reservoirs. GM denotes the conversion of resolved APE into subgrid-scale KE (mesoscale eddy parameterisation), MM stands for the transfer of resolved KE into subgrid-scale KE (momentum mixing), and RD refers to the rotated Redi diffusion that controls the conversion of both resolved APE and subgrid-scale KE into subgrid-scale APE.

is usually constrained in models using a turbulent KE (TKE) budget. In contrast, RD acts as a net transfer of energy into unresolved APE, which must balance the diffusive dissipation rate ε_p^t. This suggests that RD schemes should be constrained by a turbulent APE budget rather than by TKE. While such ideas have long been promoted in the atmospheric community (Zilitinkevich et al., 2013), they have not yet been systematically applied in ocean modelling.

The energetic significance of the APE budget lies in linking the turbulent density flux to ε_p^t and thereby to the diapycnal diffusivity K_v. In the classical relation

$$K_v \approx \frac{\varepsilon_p^t}{\overline{N}^2} = \frac{\Gamma \varepsilon_k^t}{\overline{N}^2}, \tag{1}$$

(Oakey, 1982; Gargett and Holloway, 1984; Lindborg and Brethouwer, 2008), the dissipation ratio $\Gamma = \varepsilon_p^t/\varepsilon_k^t$ measures the mixing efficiency and is often taken to be a near-constant $\Gamma \approx 0.2$. However, it is now well established that Γ depends sensitively on the turbulence regime (Salehipour and Peltier, 2015; Maffioli et al., 2016; Gregg, 2021). It can even be negative under double-diffusive instabilities (Middleton and Taylor, 2020; Middleton et al., 2021; Tailleux, 2024), and significantly greater than unity in buoyancy-driven turbulence (Scotti and White, 2011). This variability underscores that Eq. (1) should be regarded not as a universal closure, but as the physically rigorous starting point for linking vertical mixing to mechanical stirring.

The rigorous connection was derived by Tailleux and Roullet (2025) for a simple Boussinesq fluid with a linear equation of state. Under statistical stationarity and homogeneity, the eddy APE budget reduces to a balance between production — via conversions from eddy KE and mean APE — and dissipation:

$$C(E_k^t, E_a^t) + C(E_a^m, E_a^t) \approx \varepsilon_p^t. \tag{2}$$

Here, $C(E_k^t, E_a^t)$ represents the eddy-KE-to-eddy APE conversion, whereas $C(E_a^m, E_a^t)$ represents the mean-APE-to-eddy APE conversion, with

$$C(E_k^t, E_a^t) = -\overline{b'_\ell w'} = \frac{g}{\rho_\star}\overline{\rho' w'} \tag{3}$$

where $b_\ell = -(g/\rho_\star)(\rho - \rho_0(z))$, and

$$C(E_a^m, E_a^t) = -\overline{\rho' \mathbf{v}'} \cdot \nabla Y_m = -\frac{g}{\rho_\star}\overline{\rho' w'} + \frac{g}{\rho_\star}\frac{\partial z_0}{\partial \rho}(\overline{\rho})\,\overline{\rho' \mathbf{v}'} \cdot \nabla \overline{\rho}, \tag{4}$$

where $Y_m = g(z - z_0(\overline{\rho}))/\rho_\star$ (Tailleux and Roullet, 2025). With $\rho_0(z)$ the Lorenz reference density and $z_0(\rho)$ its inverse function, the contributions involving $\overline{\rho' w'}$ cancel, leaving the key balance

$$\frac{g}{\rho_\star}\frac{\partial z_0}{\partial \rho}(\overline{\rho})\,\overline{\rho' \mathbf{v}'} \cdot \nabla \overline{\rho} \approx \varepsilon_p^t. \tag{5}$$

If the turbulent density flux is parameterised as a sum of downgradient and skew components,

$$\overline{\rho' \mathbf{v}'} = -K_\rho \nabla \overline{\rho} + \boldsymbol{\Psi} \times \nabla \overline{\rho}, \tag{6}$$

with $\boldsymbol{\Psi}$ a streamfunction vector, then substitution into (5) shows that the TAPE budget constrains only the downgradient diffusivity K_ρ, leaving the skew component $\boldsymbol{\Psi}$ unconstrained:

$$-\frac{g}{\rho_\star}\frac{\partial z_0}{\partial \rho}(\overline{\rho}) K_\rho |\nabla \overline{\rho}|^2 \approx \varepsilon_p^t. \tag{7}$$

This implies

$$K_\rho = \frac{1}{\Lambda(1 + |\mathbf{S}|^2)}\frac{\varepsilon_p^t}{\overline{N}^2}, \tag{8}$$

where $|\mathbf{S}|$ measures isopycnal slope and Λ is the ratio

$$\Lambda = \frac{\partial z_0}{\partial \rho}(\overline{\rho})\frac{\partial \overline{\rho}}{\partial z} = \frac{N_0^2(\overline{\rho})}{\overline{N}^2}, \qquad \text{with} \qquad \overline{N}^2 = -\frac{g}{\rho_\star}\frac{\partial \overline{\rho}}{\partial z}. \tag{9}$$

The standard expression (1) is recovered when $\Lambda \approx 1$ and $|\mathbf{S}| \ll 1$. Thus (8) shows that departures from the Lorenz reference state directly modify the link between ε_p^t and diapycnal diffusivity — a subtle but important point rarely emphasised in past work, and one that reinforces the turbulent APE budget as the natural framework for constraining vertical mixing.

3. Energetics constraints on lateral stirring directions

The main aim of this section is to generalise the results of Tailleux and Roullet (2025) to a thermobaric ocean with a nonlinear equation of state. Prior to this, we find it useful to first discuss the relationship between Lorenz reference density (LRD) surfaces and approximately neutral surfaces (ANS), with the aim of empirically establishing the close similarities between the two concepts.

3.1. LRD surfaces versus approximately neutral surfaces (ANS)

Although it is widely accepted that the turbulent APE dissipation rate ε_p^t controls irreversible (diapycnal) mixing across density-like surfaces, the precise definition of such surfaces in a compressible, thermobaric, two-component fluid such as seawater has remained ambiguous. In the APE-based Boussinesq theory of turbulent stratified mixing, the natural candidates are Lorenz reference density (LRD) surfaces. In contrast, physical oceanography has traditionally defined "isopycnal" directions using (approximately) neutral surfaces (ANS) (Ivers, 1975; McDougall, 1987a; Jackett and McDougall, 1997).

These views are not necessarily incompatible. First, LRD surfaces can be regarded as a particular class of ANS that is close to neutral throughout most of the ocean interior (Tailleux, 2016a). Second, most ANS constructions only require neutrality in a heuristic sense, typically by minimising some measure of non-neutrality subject to practical constraints. Consequently, existing empirical ANS depend on investigator choices and optimisation criteria. LRD surfaces differ in this respect: their departure from neutrality is controlled by physics rather than by an imposed heuristic, and they arise as an emergent property of the governing equations of oceanic motions. On this basis, we propose (at least for now) to interpret existing empirical ANS as approximations to LRD surfaces, thereby unifying both concepts within the APE framework.

Our objective here is to assess how well such empirical constructs approximate LRD surfaces, focusing on two widely used ANS: the neutral density γ^n of Jackett and McDougall (1997), and the Ω surfaces introduced by Klocker et al. (2009) and subsequently refined by Stanley et al. (2021), Lang et al. (2023).

A key conceptual shift motivated by the present theory is the interpretation of non-neutrality. Historically, departures from neutrality have often been treated as "errors" to be minimised. By contrast, we argue that these departures can be viewed as signatures of thermobaric forces. In this perspective, the magnitude of thermobaric effects is proportional to the degree of non-neutrality of LRD surfaces and should therefore be regarded as a genuine physical signal rather than as a purely methodological defect.

Construction of LRD surfaces. To clarify what controls the non-neutrality of LRD surfaces, it is useful to recall how they are defined. Constructing LRD surfaces requires specification of a Lorenz reference state through reference profiles $p_0(z)$ and $\rho_0(z) = -p_0'(z)/g$ (e.g. Saenz et al., 2015). An LRD surface is the equivalence class of parcels sharing the same reference depth $z_r(S,\theta)$, obtained as the solution of the level-of-neutral-buoyancy (LNB) equation

$$\rho(S, \theta, p_0(z_r)) = \rho_0(z_r), \tag{10}$$

(Tailleux, 2013).

We regard $z_r(S,\theta)$ as the most fundamental labelling of LRD surfaces. It has three practical advantages: (i) it is naturally expressed in depth units; (ii) it is bounded in $[-H_{\max}, 0]$ (with $H_{\max}$ the maximum ocean depth), so the label set remains invariant under climate change; and (iii) it avoids the continual creation of progressively lighter density classes that can complicate density-coordinate frameworks and the interpretation of "heave" under global warming (Huang, 2020). In addition, z_r underpins objective definitions of potential vorticity (Morel et al., 2023), connects directly with quasi-geostrophic PV, and improves spice/heave decompositions relevant to ocean heat uptake (Lee et al., 2025). Any monotonic function $f(z_r)$ can serve as an alternative label; in particular, Tailleux (2016a) introduced the thermodynamic neutral density $\gamma^T(z_r)$ as a density-like label for LRD surfaces, constructed to resemble γ^n as closely as possible.

Analytical prediction of non-neutrality. Directions defined by z_r are normal to the vector

$$\mathbf{n}_r = \alpha_r \nabla\theta - \beta_r \nabla S,$$

where $\alpha_r = \alpha(S, \theta, p_r)$ and $\beta_r = \beta(S, \theta, p_r)$. This differs from the classical neutral vector $\mathbf{n} = \alpha\nabla\theta - \beta\nabla S$ only through the use of the reference pressure p_r instead of the in-situ pressure p. The misalignment between $\mathbf{n}$ and $\mathbf{n}_r$ can be written as

$$\begin{aligned} \mathbf{n} \times \mathbf{n}_r &= \beta\beta_r\left(\frac{\alpha}{\beta} - \frac{\alpha_r}{\beta_r}\right)\nabla S \times \nabla\theta \\ &= \beta\beta_r \int_{p_r}^{p} \frac{T_b}{\beta}(S, \theta, p')\,\mathrm{d}p'\,\nabla S \times \nabla\theta \\ &= \frac{\beta\beta_r \overline{T}_b (p - p_r)}{\overline{\beta}}\nabla S \times \nabla\theta, \end{aligned} \tag{11}$$

in terms of the thermobaric parameter

$$T_b = \frac{\partial \alpha}{\partial p} - \frac{\alpha}{\beta}\frac{\partial \beta}{\partial p} = \beta \frac{\partial}{\partial p}\left(\frac{\alpha}{\beta}\right), \tag{12}$$

(McDougall, 1987b; Tailleux, 2016b; Tailleux and Wolf, 2023).

Eq. (11) shows that departures from neutrality increase with (1) the distance $|p - p_r|$ between in-situ and reference pressures, and (2)

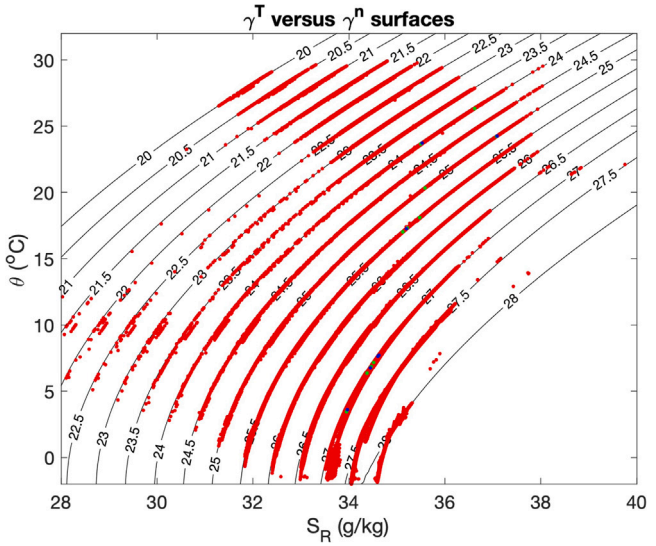

Fig. 3. Comparison of thermodynamic neutral density γ^T (black solid lines) and empirical neutral density γ^n (red dots) in (S,θ) space. The red dots correspond to (S,θ) values interpolated on selected γ^n iso-surfaces for each latitude/longitude where they are well defined.

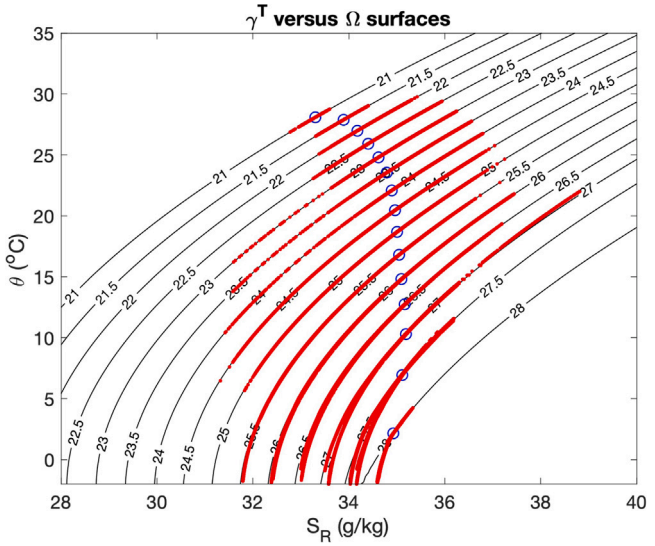

Fig. 4. Comparison of thermodynamic neutral density γ^T (black solid lines) and Ω surfaces (red dots) in (S,θ) space. The Ω surfaces plotted were chosen to intersect the γ^T isolines at the (S,θ) values marked by blue circles. The red dots correspond to (S,θ) values interpolated on the selected Ω surfaces for each latitude/longitude where they are well defined.

the misalignment of isothermal and isohaline surfaces (through $\nabla S \times \nabla\theta$). Therefore, in large parts of the ocean interior where $|p-p_r|$ is small, LRD surfaces are expected to align closely with conventional neutral approximations and thermobaric effects are weak. Conversely, in regions such as the Southern Ocean where $|p-p_r|$ can be large, thermobaricity makes accurate neutrality difficult not only for LRD surfaces, but also for any empirical ANS.

Empirical comparison in (S,θ) space. The thermodynamic neutral density $\gamma^T(S,\theta)$ is a mathematically well-defined quasi-material function of (S,θ), valid over the full physically relevant range. By contrast, γ^n and Ω surfaces are not strictly functions of (S,θ) alone, since their construction involves geographical position and pressure. This additional dependence is often assumed to be weak (McDougall and Jackett, 2005b; deSzoeke and Springer, 2009; Lang et al., 2020), but it can be assessed empirically.

To do so, we compare selected γ^n and Ω surfaces with their closest γ^T counterparts using the climatological WOCE dataset (Gouretski and Koltermann, 2004). Figs. 3 and 4 show scatter plots of all (S,θ) values extracted on chosen γ^n and Ω surfaces against the corresponding γ^T isolines, computed following Tailleux (2021). The results indicate that both γ^n and Ω capture the same overall structure as γ^T, with the largest departures occurring in the coldest waters. Scatter around γ^T isolines provides a measure of non-materiality: it is more pronounced for γ^n, while Ω surfaces tend to appear smoother but can exhibit multi-valued behaviour. Overall, these comparisons support the empirical validity of treating LRD surfaces as the underlying physical basis of present best-practice ANS.

We emphasise, however, that significant differences should not be interpreted as automatically implying that γ^n or Ω are inferior. Indeed, one cannot exclude the possibility that incorporating momentum constraints within APE theory (still under development) may eventually motivate refined isopycnal definitions that alter the relationship between physically motivated and empirically constructed surfaces.

3.2. Energetics constraints on rotated diffusion

Having established empirically that LRD surfaces provide a plausible physical basis for current best-practice ANS, we now seek theoretical support for this interpretation by extending the Boussinesq energetics argument to a thermobaric ocean with a realistic nonlinear equation of state. Our main goal is to show that the turbulent APE budget provides the fundamental constraint on the lateral stirring directions used in rotated diffusion tensors. This, in turn, further supports the idea that LRD surfaces constitute the most appropriate present definition of oceanic isopycnal surfaces (without excluding the possibility that improved definitions may emerge in the future).

Two difficulties must be acknowledged. First, the exact mean/eddy APE decomposition of Tailleux and Roullet (2025) has not yet been generalised to a fully compressible two-component ocean. Second, the nonlinearities of the seawater equation of state complicate both the conversion terms and the APE dissipation rate ε_p^t. To retain tractability, we assume that linear and nonlinear contributions to the APE budget effectively decouple, so that constraints on stirring directions can be derived from the linear part alone. The derivations below are therefore as rigorous as these assumptions allow.

We begin with the tracer evolution equations for resolved potential temperature θ and salinity S,

$$\frac{DC}{Dt} = \nabla\cdot(\mathbf{K}\nabla C), \qquad C=\{S,\theta\}, \tag{13}$$

with a diffusion tensor decomposed into skew and rotated components,

$$\mathbf{K} = \mathbf{K}_{redi} + \mathbf{K}_{skew}, \qquad \mathbf{K}_{skew}\nabla C = -\boldsymbol{\Psi}\times\nabla C, \tag{14}$$

$$\mathbf{K}_{redi} = \underbrace{K_i\left(\mathbf{I}-\mathbf{d}\mathbf{d}^T\right)}_{\mathbf{K}_{iso}} + \underbrace{K_v\,\mathbf{k}\mathbf{k}^T}_{\mathbf{K}_{ver}}, \tag{15}$$

(Griffies, 1998; Griffies et al., 1998). Here K_i and K_v denote the isopycnal and vertical diffusivities, $\mathbf{d}$ is the unit vector normal to the (as yet unspecified) lateral stirring surfaces, and $\mathbf{k}$ is the vertical unit vector. Note here that in this paper, rotated diffusion is meant to include both isopycnal and vertical/diapycnal mixing. In the literature, rotated diffusion is sometimes meant to include only isopycnal diffusion. Eq. (13) implies turbulent tracer fluxes

$$\overline{\theta'\mathbf{v}'} = -\mathbf{K}\nabla\theta, \qquad \overline{S'\mathbf{v}'} = -\mathbf{K}\nabla S. \tag{16}$$

Algebraic details used below are provided in Appendix.

3.3. Resolved APE conversion under mixing

The conversion of resolved APE into unresolved APE can be expressed in terms of the local APE density appropriate for the primitive equations (Tailleux, 2013),

$$A(S,\theta,z) = -\int_{z_r}^{z} b_\ell(S,\theta,\tilde{z})\,\mathrm{d}\tilde{z}, \tag{17}$$

where

$$b_\ell = -\frac{g}{\rho_\star}\left(\rho(S,\theta,p_0(z)) - \rho_0(z)\right)$$

is the buoyancy relative to the Lorenz reference profile $\rho_0(z)$, and z_r is the reference position of the parcel, defined by $b_\ell(S,\theta,z_r)=0$. Taking the material derivative yields

$$\frac{DA}{Dt} = -b_\ell w + \frac{\partial A}{\partial S}\frac{DS}{Dt} + \frac{\partial A}{\partial \theta}\frac{D\theta}{Dt}. \tag{18}$$

Substituting (13) gives

$$\frac{DA}{Dt} = -b_\ell w - \nabla\cdot\mathbf{J}_A - D_p, \tag{19}$$

where $\mathbf{J}_A$ is the diffusive flux of APE density and D_p its dissipation:

$$\mathbf{J}_A = -\mathbf{K}\left(\frac{\partial A}{\partial S}\nabla S + \frac{\partial A}{\partial \theta}\nabla\theta\right), \tag{20}$$

$$D_p = (\mathbf{K}\nabla S)\cdot\nabla\frac{\partial A}{\partial S} + (\mathbf{K}\nabla\theta)\cdot\nabla\frac{\partial A}{\partial \theta}, \tag{21}$$

see Appendix A.2. The dissipation D_p corresponds to the mean-to-eddy APE conversion $C(E_a^m, E_a^t)$. As shown in Appendix A.3, it can be separated into linear and nonlinear contributions associated with the equation of state. The linear contribution is

$$C(E_a^m, E_a^t)_{lin} = -g\,\mathbf{k}\cdot(\mathbf{K}\mathbf{n}) + \frac{g^2}{N_{0r}^2}(\mathbf{K}_{redi}\mathbf{n}_r)\cdot\mathbf{n}_r, \tag{22}$$

where $\mathbf{n}_r = \alpha_r\nabla\theta - \beta_r\nabla S$ is the neutral-like vector normal to LRD surfaces (with $\alpha_r = \alpha(S,\theta,p_r)$ and $\beta_r = \beta(S,\theta,p_r)$), and N_{0r}^2 is the reference buoyancy frequency,

$$N_0^2(S,\theta,z) = -\frac{g}{\rho_b}\left(\frac{d\rho_0}{dz}(z) + \frac{\rho_0^2(z)\,g}{\rho_b c_{sb}^2}\right), \tag{23}$$

evaluated at depth z_r.

3.4. Conversion from eddy KE to eddy APE

The eddy KE to eddy APE conversion retains its Boussinesq form,

$$C(E_k^t, E_a^t) = \frac{g}{\rho_\star}\overline{\rho' w'}. \tag{24}$$

Using the linearised density anomaly $\rho' \approx \rho_\star(\beta S' - \alpha\theta')$ and (16) gives

$$C(E_k^t, E_a^t)_{lin} = g(\beta\overline{S'w'} - \alpha\overline{\theta' w'}) = g\,\mathbf{k}\cdot(\mathbf{K}\mathbf{n}). \tag{25}$$

This exactly cancels the first term in (22), leaving the linear eddy APE budget

$$\boxed{C(E_k^t, E_a^t)_{lin} + C(E_a^m, E_a^t)_{lin} = \frac{g^2}{N_{0r}^2}(\mathbf{K}_{redi}\mathbf{n}_r)\cdot\mathbf{n}_r = \varepsilon_{p,lin}^t.} \tag{26}$$

Eq. (26) is the central theoretical result. It links the Redi tensor $\mathbf{K}_{redi}$ to the turbulent APE dissipation rate $\varepsilon_{p,lin}^t$ and, through (1), to diapycnal diffusivity. Because the skew component satisfies $(\mathbf{K}_{skew}\mathbf{n}_r)\cdot\mathbf{n}_r = 0$, the energetic constraint applies solely to the rotated diffusion component. Expanding (26) yields

$$\frac{g^2}{N_{0r}^2}(\mathbf{K}_{redi}\mathbf{n}_r)\cdot\mathbf{n}_r = \frac{g^2}{N_{0r}^2}\left[K_i|\mathbf{n}_r|^2\sin^2\widehat{(\mathbf{d},\mathbf{n}_r)} + K_v(\mathbf{k}\cdot\mathbf{n}_r)^2\right]. \tag{27}$$

Energetic consistency requires that the dissipation rate $\varepsilon_{p,lin}^t$ should not depend on the arbitrary magnitude of the isopycnal diffusivity K_i. Eq. (27) shows that such independence is possible only if

$$\mathbf{d} = \frac{\mathbf{n}_r}{|\mathbf{n}_r|}, \tag{28}$$

i.e. the lateral stirring directions must coincide with LRD surfaces.

3.5. Objective definition of the Veronis effect

If $\mathbf{d}$ is not aligned with $\mathbf{n}_r$, the rotated diffusion tensor induces a spurious (fictitious) contribution to vertical/diapycnal mixing. In the small-angle limit, this can be represented as an effective fictitious vertical diffusivity

$$K_v^f \approx K_i\sin^2\widehat{(\mathbf{d},\mathbf{n}_r)}, \tag{29}$$

so that

$$\frac{g^2}{N_{0r}^2}(\mathbf{K}_{redi}\mathbf{n}_r)\cdot\mathbf{n}_r = \frac{g^2(\mathbf{k}\cdot\mathbf{n}_r)^2}{N_{0r}^2}(K_v + K_v^f). \tag{30}$$

Eqs. (29)–(30) therefore provide a rigorous and objective definition of the Veronis effect (Veronis, 1975): fictitious vertical mixing produced by misalignment between the assumed lateral stirring directions and the physically constrained LRD directions.

3.6. Linking K_v to observed diapycnal mixing

When $\mathbf{d}$ aligns with $\mathbf{n}_r$, the linear eddy APE budget (26) reduces to

$$\frac{g^2(\mathbf{k}\cdot\mathbf{n}_r)^2}{N_{0r}^2}K_v \approx \varepsilon_{p,lin}^t = K_\rho|\Lambda|(1+|\mathbf{S}|^2)\,\overline{N}^2. \tag{31}$$

Using the identities (see Appendix)

$$\frac{g|\mathbf{k}\cdot\mathbf{n}_r|}{N_{0r}^2} = \frac{\partial z_r}{\partial z}, \qquad \Lambda = \frac{N_{0r}^2}{\overline{N}^2}, \qquad \mathbf{S} = -\left(\frac{\partial z_r}{\partial z}\right)^{-1}\nabla_h z_r, \tag{32}$$

one obtains

$$K_v = |\nabla z_r|^2\,K_\rho. \tag{33}$$

Thus, the vertical coefficient K_v appearing in the Redi tensor exceeds the observed diapycnal diffusivity K_ρ by the amplification factor $|\nabla z_r|^2$, and coincides with K_ρ only when isopycnals are flat. This clarifies the distinction between "vertical" and "diapycnal" diffusivities and shows that Redi's vertical coefficient should be interpreted as an amplified form of K_ρ, rather than as the diapycnal mixing itself.

4. Illustrative applications

4.1. Veronis effect due to isoneutral mixing

The primary consequence of our results is that mixing along neutral directions generally induces an energy transfer between APE and BPE. In a numerical ocean model, this transfer manifests as a source of spurious turbulent diapycnal mixing, which we identify as the Veronis effect. To quantify this, consider a neutral rotated diffusion tensor defined by the normalised neutral direction

$$\mathbf{d} = \frac{\mathbf{n}}{|\mathbf{n}|}. \tag{34}$$

Eq. (27) then predicts a fictitious diapycnal mixing term given by

$$K_v^{spurious} = K_i\sin^2\widehat{(\mathbf{n},\mathbf{n}_r)}, \tag{35}$$

which is closely related to the "fictitious diapycnal mixing" metric used in the neutral density literature (Hochet et al., 2019). In earlier studies (e.g. McDougall and Jackett, 2005a; Tailleux, 2016a), departures from neutrality were commonly interpreted as "errors", and metrics such as (35) were seen as fictitious mixing arising from those errors. We stress, however, that the term "error" is mathematically misleading

when applied to departures from an idealised but physically impossible concept like a perfectly neutral surface. Instead, we argue that (35) quantifies the spurious mixing introduced by isoneutral parameterisations, given that $\mathbf{n}_r$ represents the physically-based definition of lateral stirring directions.

Because diapycnal fluxes are directly linked to APE dissipation, diagnosing these contributions ideally requires exact local APE diagnostics within OGCMs. While such diagnostics are still being fully implemented and tested, we can estimate $K_v^{spurious}$ from Eq. (35) using a typical value of $K_i = 10^3\,\mathrm{m^2 s^{-1}}$, the WOCE climatology, and the $\mathbf{n}_r$ calculation method of Tailleux (2021). Fig. 5 shows the results for two transects in the Atlantic and Pacific, where white regions identify areas where $K_v^{spurious} > 10^{-5}\,\mathrm{m^2 s^{-1}}$.

The results confirm that $\mathbf{n}_r$ is nearly neutral over most of the ocean interior; in these regions, mixing along LRD surfaces is effectively equivalent to isoneutral mixing. Significant spurious contributions occur only where $|p - p_r|$ is large, most notably in the Southern Ocean. Interestingly, the Southern Ocean is precisely where numerical studies show that stratification and circulation are unexpectedly sensitive to the choice of isoneutral diffusion, as seen in Forget et al. (2015) (using the MITgcm adjoint) and Chouksey et al. (2022) (using PyOM). This sensitivity is surprising because isopycnal mixing has traditionally been viewed as having a minimal impact on stratification and potential energy (Sverdrup et al., 1942). While cabbeling and thermobaricity may contribute, our analysis suggests that the Veronis effect induced by isoneutral mixing is likely the primary cause. Given the Southern Ocean's critical role in global heat and carbon budgets, this issue requires urgent clarification.

4.2. Possible generalisations and extensions

The concept of diagnosing turbulent diapycnal mixing in simulations by studying conversions between APE and BPE — for instance, by monitoring the evolution of the Lorenz reference density profile — dates back to Winters et al. (1995). Since then, several studies have attempted to exploit this framework to diagnose spurious diapycnal mixing in ocean models (e.g., Griffies et al., 2000; Ilicak et al., 2012; Ilicak, 2016). More broadly, Butler et al. (2013) suggested characterising all resolved and unresolved processes by their tendencies in APE/BPE space. In this framework, adiabatic processes should leave the BPE unaffected, meaning their APE and PE tendencies should be identical:

$$\frac{\partial APE}{\partial t} = \frac{\partial PE}{\partial t}. \tag{36}$$

Any departure from (36) indicates the presence of spurious diapycnal mixing. Fig. 6 illustrates this methodology for the oceanic component of a coupled climate model. While resolved advection and eddy-induced advection should theoretically satisfy (36) exactly, the figure shows they only do so approximately, consistent with the known fact that numerical advection schemes introduce spurious numerical mixing.

Our results show, however, that generalising the Winters et al. (1995) framework to numerical ocean models is not straightforward. Turbulent diapycnal mixing relates to the net conversion of unresolved small-scale APE into BPE due to molecular diffusion. This paper demonstrates that such a conversion cannot be directly diagnosed solely from the impact of parameterised mixing on resolved APE. This has important practical implications: simply diagnosing the sources and sinks of APE across resolved and unresolved processes may not be sufficient to isolate spurious diapycnal mixing. This suggests that studying the evolution of the background potential energy (BPE) is a better approach. However, the exact form of the BPE for the seawater Boussinesq approximation remains to be fully clarified. Furthermore, LRD surfaces can exhibit inversions, particularly in the Southern Ocean, which complicates these diagnostics. We hypothesise that consistently defining stirring surfaces in such cases will require the inclusion of momentum constraints. Extensions of this theory in simplified contexts are already under development (Codoban and Shepherd, 2003, 2006;

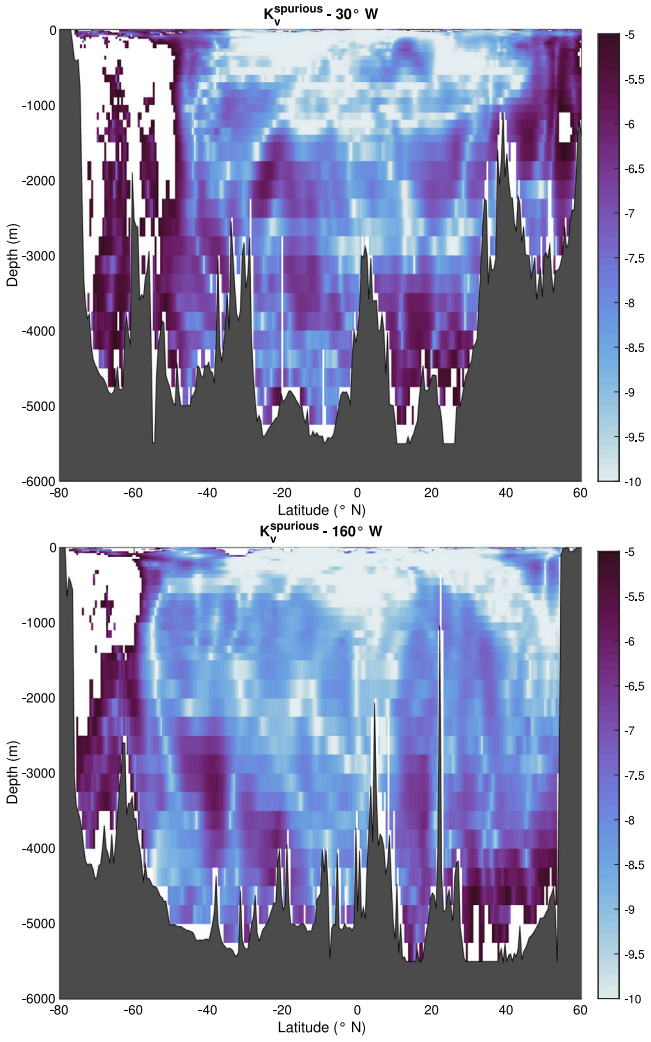

Fig. 5. Spurious diapycnal mixing associated with neutral directions in the rotated diffusion tensor. White shading identifies regions where $K_v^{spurious} > 10^{-5}\,\mathrm{m^2\,s^{-1}}$ along two transects in the Pacific and Atlantic.

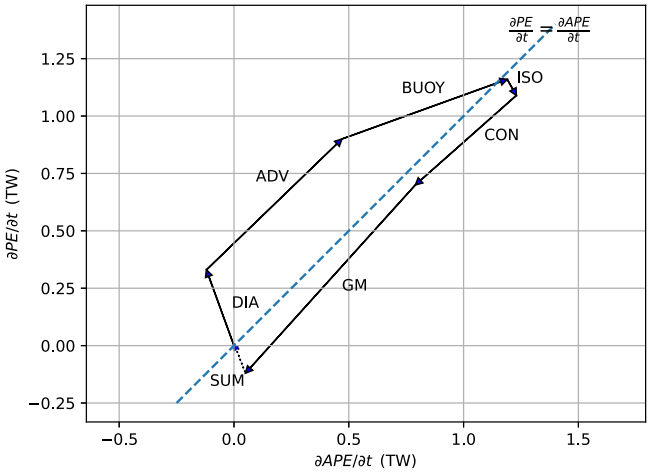

Fig. 6. Contributions of resolved and unresolved physical processes to the energetics of a numerical ocean general circulation model in APE/PE space. Adapted from Butler et al. (2013). DIA = turbulent diapycnal mixing; ADV = resolved advection; BUOY = surface buoyancy forcing including penetrative solar heating; ISO = isoneutral mixing; CON = convective adjustment; GM = Gent-McWilliams eddy-induced advection; SUM = residual.

Andrews, 2006; Scotti and Passagia, 2019; Harris and Tailleux, 2025) and may eventually unify isentropic and isopycnic perspectives across geophysical fluids. Implementing practical APE diagnostics, even in simplified forms using a fixed reference profile $\rho_0(z)$ — such as the one underlying the thermodynamic neutral density of Tailleux (2016a) — remains computationally expensive. Further research is needed to make these methods efficient for climate applications, a topic we will address in future work.

5. Summary and conclusions

This paper shows that the turbulent available potential energy (TAPE) budget, rather than the turbulent kinetic energy (TKE) budget, provides the appropriate energetic framework for constraining the lateral stirring directions entering rotated (Redi) diffusion tensors in seawater. The key reason is that the choice of lateral directions directly controls the production of turbulent APE by rotated diffusion. Energetic consistency therefore requires that this production be balanced by the turbulent APE dissipation rate ϵ_p^t, which sets the diapycnal diffusivity K_ρ. If the stirring directions are chosen inconsistently with this constraint, the TAPE production becomes spuriously sensitive to the (often large) isopycnal diffusivity K_i, giving rise to the long-recognised but previously ill-defined Veronis effect (Veronis, 1975).

Within the present framework, this ambiguity is resolved: the Veronis effect is identified as fictitious vertical (diapycnal) mixing induced by misalignment between the assumed lateral stirring directions and the energetically constrained ones. We show that the only choice that removes the spurious dependence on K_i is to define lateral stirring along Lorenz reference density (LRD) surfaces, i.e. the isosurfaces of the reference state central to APE theory. With this choice, the production of turbulent APE by rotated diffusion becomes controlled by physical diapycnal processes rather than by arbitrary large lateral diffusivities, thereby eliminating the Veronis effect.

The paper further clarifies the relationship between model mixing coefficients and observable measures of turbulence. In particular, by linking the TAPE budget to ϵ_p^t and hence to K_ρ, the theory explains how the "vertical" diffusivity K_v appearing in the Redi tensor relates to the observed diapycnal diffusivity. In general, these quantities differ: K_v should be interpreted as an amplified form of K_ρ, with amplification determined by the geometry of LRD surfaces (reducing to equality only when isopycnals are flat). This provides a concrete interpretation of why apparently "vertical" coefficients in rotated diffusion parameterisations should not be equated directly with diapycnal mixing.

Our results also shed new light on the long-standing question of what empirical approximately neutral surfaces (ANS) are approximating. Comparisons in (S,θ) space show that empirical ANS such as γ^n and Ω surfaces largely follow the structure of the thermodynamic neutral density γ^T (a density-like labelling of LRD surfaces), diverging primarily in the coldest waters. In this view, LRD surfaces emerge as the underlying physical object that ANS constructions attempt to emulate. Importantly, departures from neutrality are not treated here as "errors" to be minimised, but as signatures of thermobaric forces, i.e. a real physical effect that becomes large where the distance $|p-p_r|$ from the reference pressure is large and where ∇S and $\nabla\theta$ are strongly misaligned.

A direct implication is that constructing rotated diffusion using classical neutral directions is unphysical in a thermobaric ocean: it introduces spurious diapycnal mixing through the Veronis effect, potentially most significant in the Southern Ocean. This is noteworthy because the Southern Ocean is also the region where OGCM studies report unexpectedly strong sensitivity of stratification and circulation to isoneutral diffusion (Forget et al., 2015; Chouksey et al., 2022), despite the long-standing expectation that isopycnal/isoneutral stirring should minimally affect stratification and potential energy (Sverdrup et al., 1942). Distinguishing between genuine physical effects (e.g. cabbeling and thermobaricity) and numerical artefacts associated with spurious diapycnal mixing is therefore crucial for reliable projections of heat and carbon uptake.

Finally, the present results highlight practical priorities for future work. First, diagnosing spurious diapycnal mixing in OGCMs will likely require implementing local APE diagnostics, because the net conversion of unresolved APE into background potential energy by molecular diffusion cannot, in general, be inferred solely from tendencies of resolved APE. Second, the use of LRD surfaces as stirring directions raises conceptual questions about the locality of the Lorenz reference state. For LRD-based stirring to remain compatible with the assumed locality of lateral mixing closures, it may be necessary for the Lorenz reference state to behave as a local environmental property, as recently discussed by Tailleux (2025); this point remains controversial and merits further investigation.

In summary, by identifying LRD surfaces as the energetically consistent lateral stirring surfaces for rotated diffusion (as first hypothesised by Tailleux (2016a)), this work provides a physically grounded pathway for reducing or eliminating spurious diapycnal mixing, improving energetic consistency of ocean mixing parameterisations, and strengthening the foundations of both isopycnal and z-coordinate modelling frameworks within the unified perspective of APE theory.

Declaration of competing interest

The authors declare that they have no known competing financial interests or personal relationships that could have appeared to influence the work reported in this paper.

Acknowledgements

The author thank Stephen Griffies for extensive comments on a previous version of this manuscript, as well as two anonymous reviewers. The author also acknowledges discussions with Geoff Stanley and Trevor McDougall over the years, which helped identifying the issues to be solved. This research has been partially supported by the Natural Environment Research Council (NERC)-funded OUTCROP project (grant no. NE/R010536/1).

Appendix. Impact of mixing parameterisations on APE budget

The local APE density for two-component seawater in the standard Boussinesq approximation can be expressed as:

$$A(S,\theta,z) = -\int_{z_r}^{z} b_{\ell'}(S,\theta,\tilde{z})\,\mathrm{d}\tilde{z}, \tag{A.1}$$

(Tailleux, 2013). Here, $b_{\ell'}$ is the buoyancy defined relative to the Lorenz reference density profile $\rho_0(z)$. Conventionally, this buoyancy is expressed as:

$$b_{\ell'} = -\frac{g(\rho-\rho_0(z))}{\rho_\star}, \tag{A.2}$$

where g is the gravitational acceleration, ρ is the in-situ density, and $\rho_\star$ is a (constant) reference density. Alternatively, a more accurate form of buoyancy is:

$$b_{\ell'}(S,\theta,z) = -g\left[1-\rho_0(z)v(S,\theta,p_0(z))\right] = -g[1-\rho_0(z)v_b], \tag{A.3}$$

(Young, 2012; Tailleux, 2012; Tailleux and Dubos, 2024) where the subscript b indicates thermodynamic quantities evaluated at the reference pressure $p_0(z)$ rather than the actual pressure p. Eq. (A.3) has the advantage of allowing the APE density to be expressed in terms of thermodynamic potentials developed as part of the new equation of state IOC et al. (2010), viz.,

$$A(S,\theta,z) = h(S,\theta,p_0(z)) - h(S,\theta,p_0(z_r)) + g(z-z_r), \tag{A.4}$$

where $h(S,\theta,p)$ is the specific enthalpy (Tailleux and Dubos, 2024).

The reference position $z_r = z_r(S,\theta)$ is determined as the solution to the Level of Neutral Buoyancy (LNB) equation:

$$b_\ell(S,\theta,z_r) = 0, \tag{A.5}$$

as originally shown by Tailleux (2013).

A.1. Derivatives of buoyancy and APE density

Before deriving the evolution equation for the local APE density A, it is useful to compute the thermohaline and vertical derivatives of buoyancy, as these define the thermal expansion coefficient α, haline contraction coefficient β, and the reference squared buoyancy frequency profile $N_0^2(S,\theta,z)$. These derivatives are given by:

$$\frac{\partial b_\ell}{\partial S} = g\rho_0(z)\frac{\partial \upsilon_b}{\partial S} = -g\beta(S,\theta,z), \tag{A.6}$$

$$\frac{\partial b_\ell}{\partial \theta} = g\rho_0(z)\frac{\partial \upsilon_b}{\partial \theta} = g\alpha(S,\theta,z), \tag{A.7}$$

$$\frac{\partial b_\ell}{\partial Z} = \frac{g}{\rho_b}\left(\frac{d\rho_0}{dz} + \frac{\rho_0^2(z)g}{\rho_b c_{sb}^2}\right) = -N_0^2(S,\theta,z), \tag{A.8}$$

where $\partial/\partial Z$ denotes partial differentiation with respect to z at fixed (S,θ), while $\partial/\partial z$ refers to differentiation at fixed (x,y,t).

Using these expressions, the thermohaline derivatives of the reference depth z_r can be obtained by taking the total differential of the LNB Eq. (A.5):

$$\frac{\partial b_\ell}{\partial S}\mathrm{d}S + \frac{\partial b_\ell}{\partial \theta}\mathrm{d}\theta + \frac{\partial b_\ell}{\partial Z}\mathrm{d}z_r = 0. \tag{A.9}$$

This leads to the following expressions for the thermohaline derivatives of z_r:

$$\frac{\partial z_r}{\partial S} = -\frac{g\beta_r}{N_0^2(S,\theta,z_r)} = -\frac{g\beta_r}{N_{0r}^2}, \tag{A.10}$$

$$\frac{\partial z_r}{\partial \theta} = \frac{g\alpha_r}{N_0^2(S,\theta,z_r)} = \frac{g\alpha_r}{N_{0r}^2}, \tag{A.11}$$

where the subscript r denotes quantities evaluated at the reference depth z_r. It follows that

$$\nabla z_r = \frac{g(\alpha_r\nabla\theta - \beta_r\nabla S)}{N_{0r}^2}. \tag{A.12}$$

In the text, we also introduced the additional reference squared buoyancy frequency

$$N_{1r}^2 = g\left(\alpha_r\frac{\partial\theta}{\partial z} - \beta_r\frac{\partial S}{\partial z}\right). \tag{A.13}$$

Eq. (A.12) shows that N_{1r}^2 and N_{0r}^2 differ from each other, being related through

$$\frac{N_{1r}^2}{N_{0r}^2} = \frac{\partial z_r}{\partial z}. \tag{A.14}$$

The derivatives of the APE density A are then given by:

$$\frac{\partial A}{\partial S} = g\int_{z_r}^{z}\beta(S,\theta,\tilde{z})\,\mathrm{d}\tilde{z}, \tag{A.15}$$

$$\frac{\partial A}{\partial \theta} = -g\int_{z_r}^{z}\alpha(S,\theta,\tilde{z})\,\mathrm{d}\tilde{z}, \tag{A.16}$$

$$\frac{\partial A}{\partial Z} = -b_\ell. \tag{A.17}$$

For convenience, we define:

$$Y_S = \frac{\partial A}{\partial S}, \quad Y_\theta = \frac{\partial A}{\partial \theta}, \tag{A.18}$$

to emphasise the thermodynamic efficiency-like character of these derivatives.

A.2. Evolution equation for APE density

The evolution equation for the local APE density can be written as:

$$\frac{DA}{Dt} = -b_\ell w + Y_S\frac{DS}{Dt} + Y_\theta\frac{D\theta}{Dt}. \tag{A.19}$$

Substituting $\frac{DS}{Dt} = \nabla\cdot(\mathbf{K}\nabla S)$ and $\frac{D\theta}{Dt} = \nabla\cdot(\mathbf{K}\nabla\theta)$, this becomes:

$$\frac{DA}{Dt} = -b_\ell w - \nabla\cdot\mathbf{J}_A - D_p, \tag{A.20}$$

where $\mathbf{J}_A$ is the turbulent diffusive flux of APE density, and D_p is the net conversion rate of mean APE and eddy APE. These are given by:

$$\mathbf{J}_A = -Y_S\mathbf{K}\nabla S - Y_\theta\mathbf{K}\nabla\theta = -\mathbf{K}\mathbf{P}_a, \tag{A.21}$$

$$D_p = (\mathbf{K}\nabla S)\cdot\nabla Y_S + (\mathbf{K}\nabla\theta)\cdot\nabla Y_\theta, \tag{A.22}$$

where $\mathbf{P}_a = Y_S\nabla S + Y_\theta\nabla\theta$ is an APE-based form of the P-vector, as discussed by Nycander (2011) and further developed in Tailleux and Wolf (2023).

A.3. Linear and nonlinear contributions to D_p

The term D_p can be decomposed into linear and nonlinear contributions:

$$D_p = D_p^L + D_p^{NL}, \tag{A.23}$$

where the linear part is:

$$D_p^L = \frac{g^2}{N_{0r}^2}(\mathbf{K}\mathbf{n}_r)\cdot\mathbf{n}_r - g\mathbf{k}\cdot(\mathbf{K}\mathbf{n}), \tag{A.24}$$

and the nonlinear part is:

$$\begin{aligned} D_p^{NL} = &-\int_{z_r}^{z} b_{SS}\,\mathrm{d}z'(\mathbf{K}\nabla S)\cdot\nabla S - \int_{z_r}^{z} b_{\theta\theta}\,\mathrm{d}z'(\mathbf{K}\nabla\theta)\cdot\nabla\theta \\ &- 2\int_{z_r}^{z} b_{S\theta}\,\mathrm{d}z'(\mathbf{K}\nabla S)\cdot\nabla\theta. \end{aligned} \tag{A.25}$$

Alternatively, this can be expressed as:

$$D_p^{NL} = -(z-z_r)\left[\overline{b_{SS}}(\mathbf{K}\nabla S)\cdot\nabla S + 2\overline{b_{S\theta}}(\mathbf{K}\nabla\theta)\cdot\nabla S + \overline{b_{\theta\theta}}(\mathbf{K}\nabla\theta)\cdot\nabla\theta\right], \tag{A.26}$$

where the overbar denotes an average over $[z_r, z]$.

Data availability

Data will be made available on request.

References

Andrews, D.G., 2006. On the available energy density for axisymmetric motions of a compressible stratified fluid. J. Fluid Mech. 569, 481–492.

Butler, E.D., Oliver, K.I.C., Gregory, J.M., Tailleux, R., 2013. The ocean's gravitational potential energy budget in a coupled climate model. Geophys. Res. Lett. 40, 5417–5422.

Chouksey, A., Griesel, A., Chouksey, M., Eden, C., 2022. Changes in global ocean circulation due to isopycnal diffusion. J. Phys. Oceanogr. 52, 2219–2235. http://dx.doi.org/10.1175/JPO-D-21-0205.1.

Codoban, S., Shepherd, T.G., 2003. Energetics of a symmetric circulation including momentum constraints. J. Atmos. Sci. 60, 2019–2028.

Codoban, S., Shepherd, T.G., 2006. On the available energy of an axisymmetric vortex. Meteo. Z. 15, 401–407.

deSzoeke, R.A., Springer, S.R., 2009. The materiality and neutrality of neutral density and orthobaric density. J. Phys. Oceanogr. 39, 1779–1799. http://dx.doi.org/10.1175/2009JPO4042.1.

Eden, C., 2015. Revisiting the energetics of the ocean in Boussinesq approximation. J. Phys. Oceanogr. 45, 630–637.

Eden, C., 2016. Closing the energy cycle in an ocean model. Ocean. Model. 101, 30–42.

Eden, C., Czeschel, L., Olbers, D., 2014. Toward energetically consistent ocean models. J. Phys. Oceanogr. 44, 3160–3184. http://dx.doi.org/10.1175/JPO-D-13-0260.1.

Forget, G., Ferrerira, D., Liang, X., 2015. On the observability of turbulent transport rates by argo: supporting evidence from an inversion experiment. Ocean. Sci. 11, 839–853.

Gargett, A.E., Holloway, G., 1984. Dissipation and diffusion by internal wave breaking. J. Mar. Res. 42, 15–27.

Gent, P., McWilliams, J.C., 1990. Isopycnal mixing in ocean circulation models. J. Phys. Oceanogr. 20, 150–155.

Gent, P., Willebrand, J., McDougall, T.J., McWilliams, J.C., 1995. Parameterizing eddy-induced tracer transports in ocean circulation models. J. Phys. Oceanogr. 25, 463–474.

Gouretski, V.V., Koltermann, K.P., 2004. WOCE Global Hydrographic Climatology. Berichte des Bundesamtes für Seeshifffahrt und Hydrographie Tech. Rep. 35/2004, 49pp.

Gregg, M.C., 2021. Ocean Mixing. Cambridge University Press.

Griffies, S.M., 1998. The gent-mcwilliams skew flux. J. Phys. Oceanogr. 28, 831–841. http://dx.doi.org/10.1175/1520-0485(1998)028%3C0831{:}TGMSF%3E2.0.CO{;}2.

Griffies, S.M., Gnanadesikan, A., Pacanowski, R.C., Larichev, V.D., Dukowicz, J.K., Smith, R.D., 1998. Isoneutral diffusion in a z-coordinate ocean model. J. Phys. Oceanogr. 28, 805–830. http://dx.doi.org/10.1175/1520-0485(1998)028%3C0805{:}IDIAZC%3E2.0.CO{;}2.

Griffies, S.M., Pacanowski, R.C., Hallberg, R.W., 2000. Spurious diapycnal mixing associated with advection in a z-coordinate ocean model. Mon. Wea. Rev. 128, 538–564. http://dx.doi.org/10.1175/1520-0493(2000)128%3C0538{:}SDMAWA%3E2.0.CO{;}2.

Harris, B.L., Tailleux, R., 2025. Diabatic and frictional controls of an axisymmetric vortex using available potential energy theory with a non-resting state. Atmosphere 16, 700. http://dx.doi.org/10.3390/atmos16060700.

Hochet, A., Tailleux, R., Ferreira, D., Kuhlbrodt, T., 2019. Isoneutral control of effective diapycnal mixing in numerical ocean models with neutral rotated diffusion tensors. Ocean. Sci. 15, 21–32. http://dx.doi.org/10.5194/os-15-21-2019.

Huang, R.X., 2020. Heaving, Stretching and Spicing Modes: Climate Variability in the Ocean. Springer Nature.

Ilicak, M., 2016. Quantifying spatial distribution of spurious mixing in ocean models. Ocean. Model. 108, 30–38. http://dx.doi.org/10.1016/j.ocemod.2016.11.002.

Ilicak, M., Adcroft, A., Griffies, S.M., Hallberg, R., 2012. Spurious dianeutral mixing and the role of momentum closure. Ocean. Model. 45–46, 37–58.

IOC, SCOR, IAPSO, 2010. The international thermodynamic equation of seawater - 2010: Calculation and use of thermodynamic properties. Manual and Guides No. 56, Intergovernmental Oceanographic Commision, UNESCO (English).

Ivers, W.D., 1975. The Deep Circulation in the Northern North Atlantic, with Especial Reference To the Labrador Sea (Ph.D. thesis). Scripps Institute of Oceanography, University of California, San Diego.

Jackett, D.R., McDougall, T.J., 1997. A neutral density variable for the world's oceans. J. Phys. Oceanogr. 27, 237–263. http://dx.doi.org/10.1175/1520-0485(1997)027<0237:ANDVFT>2.0.CO;2.

Klocker, A., McDougall, T.J., Jackett, D.R., 2009. A new method for forming approximately neutral surfaces. Ocean. Sci. 5, 155–172. http://dx.doi.org/10.5194/os-5-155-2009.

Lang, Y., Stanley, G.J., McDougall, T.J., 2023. Spurious dianeutral advection and methods for its minimization. J. Phys. Oceanogr. http://dx.doi.org/10.1175/JPO-D-22-0174.1.

Lang, Y., Stanley, G.J., McDougall, T.J., Barker, P., 2020. A pressure-invariant neutral density variable for the world's oceans. J. Phys. Oceanogr. 50, 3585–3604. http://dx.doi.org/10.1175/JPO-D-19-0321.1.

Lee, J., Tailleux, R., Kuhlbrodt, T., 2025. Disantangling anthropogenic and dynamic contributions to recent ocean warming. Npj Clim Atmos Sci 8, http://dx.doi.org/10.1038/s41612-025-01043-7.

Lemarié, F., Debreu, L., Shchepetkin, A.F., McWilliams, J.C., 2012. On the stability and accuracy of the harmonic and biharmonic isoneutral mxiing operators in ocean models. Ocean. Model. 52–53, 9–35. http://dx.doi.org/10.1016/j.ocemod.2012.04.007.

Lindborg, E., Brethouwer, G., 2008. Vertical dispersion by stratified turbulence. J. Fluid Mech. 614, 303–314.

Lorenz, E.N., 1955. Available potential energy and the maintenance of the general circulation. Tellus 7, 157–167.

Lynn, R.J., Reid, J.L., 1968. Characteristics and circulation of deep and abyssal waters. Deep. Sea Res. 15, 577–598. http://dx.doi.org/10.1016/0011-7471(68)90064-8.

Maffioli, A., Brethouwer, G., Lindborg, E., 2016. Mixing efficiency in stratified turbulence. J. Fluid Mech. 794.

Mak, J., Maddison, J.R., Marshall, D.P., Munday, D.R., 2018. Implementation of a geometrically informed and energetically constrained mesoscale eddy parameterization in an ocean circulation model. J. Phys. Oceanogr. 48, 2363–2382.

Marshall, D.P., Maddison, J.R., Berloff, P.S., 2012. A framework for parameterising eddy potential vorticity fluxes. J. Phys. Oceanogr. 42, 539–557.

McDougall, T.J., 1987a. Neutral surfaces. J. Phys. Oceanogr. 17, 1950–1964.

McDougall, T.J., 1987b. Thermobaricity, cabbeling, and water mass-conversion. J. Geophys. Res. Ocean. 92, 5448–5464.

McDougall, T.J., Church, J.A., 1986. Pitfalls with the numerical representation of isopycnal diapycnal mixing. J. Phys. Oceanogr. 16, 196–199.

McDougall, T.J., Groeskmap, S., Griffies, S.M., 2014. On geometrical aspects of interior ocean mixing. J. Phys. Oceanogr. 44, 2164–2175.

McDougall, T.J., Jackett, D.R., 2005a. An assessment of orthobaric density in the global ocean. J. Phys. Oceanogr. 35, 2054–2075.

McDougall, T.J., Jackett, D.R., 2005b. The material derivative of neutral density. J. Mar. Res. 63, 159–185.

Middleton, L., Fine, E.C., MacKinnon, J.A., Alford, M.H., Taylor, J.R., 2021. Estimating dissipation rates associated with double diffusion. Geophis. Res. Lett. 48, http://dx.doi.org/10.1029/2021GL092779.

Middleton, L., Taylor, J.R., 2020. A general criterion for the release of background potential energy through double diffusion. J. Fluid Mech. 893.

Morel, Y., Morvan, G., Benshila, R., Renault, L., Gula, J., Auclair, F., 2023. An "objective" definition of potential vorticity. generalized evolution equation and application to the study of coastal upwelling instability. Ocean. Model. 186, http://dx.doi.org/10.1016/j.ocemod.2023.102287.

Nycander, J., 2010. Horizontal convection with a non-linear equation of state: generalization of a theorem of Paparella and Young. Tellus 62A, 134–237.

Nycander, J., 2011. Energy conversion, mixing energy, and neutral surfaces with a nonlinear equation of state. J. Phys. Oceanogr. 41, 28–41.

Oakey, N.S., 1982. Determination of the rate of dissipation of turbulent energy from simultaneous temperature and velocity shear microstructure measurements. J. Phys. Oceanogr. 12, 256–271. http://dx.doi.org/10.1175/1520-0485(1982)012%3C0256{:}DOTROD%3E2.0.CO{;}2.

Redi, M.H., 1982. Oceanic isopycnal mixing by coordinate rotation. J. Phys. Oceanogr. 12, 1154–1158.

Saenz, J.A., Tailleux, R., Butler, E.D., Hughes, G.O., Oliver, K.I.C., 2015. Estimating Lorenz's reference state in an ocean with a nonlinear equation of state for seawater. J. Phys. Oceanogr. 45, 1242–1257. http://dx.doi.org/10.1175/JPO-D-14-0105.1.

Salehipour, H., Peltier, W.R., 2015. Diapycnal diffusivity, turbulent Prandtl number and mixing efficiency in boussinesq stratified turbulence. J. Fluid Mech. 775, 464–500.

Scotti, A., Passagia, P.Y., 2019. Diagnosing the diabatic effects on the available energy of stratified flows in inertial and non-inertial frames. J. Fluid Mech. 861, 608–642.

Scotti, A., White, B., 2011. Is horizontal convection really "non-turbulent"? Geophis. Res. Lett. 38, http://dx.doi.org/10.1029/2011GL049701.

Scotti, A., White, B., 2014. Diagnosing mixing in stratified turbulent flows with a locally defined available potential energy. J. Fluid Mech. 740, 114–135.

Solomon, H., 1971. On the representation of isentropic mixing in ocean models. J. Phys. Oceanogr. 1, 233–234.

Stanley, G.J., McDougall, T.J., Barker, P.M., 2021. Algorithmic improvements to finding approximately neutral surfaces. J. Adv. Model. Earth Syst. 13.

Sverdrup, H., Johnson, M.W., Fleming, R.H., 1942. Significance of σ_t Surfaces. Prentice-Hall, Inc. New York, pp. 414–416, URL: http://ark.cdlib.org/ark:/13030/kt167nb66r/.

Tailleux, R., 2009. On the energetics of turbulent stratified mixing, irreversible thermodynamics, boussinesq models, and the ocean heat engine controversy. J. Fluid Mech. 638, 339–382.

Tailleux, R., 2012. Thermodynamics/dynamics coupling in weakly compressible turbulent stratified fluids. ISRN Thermodyn. 2012, 609701. http://dx.doi.org/10.5402/2012/609701.

Tailleux, R., 2013. Available potential energy density for a multicomponent Boussinesq fluid with a nonlinear equation of state. J. Fluid Mech. 735, 499–518. http://dx.doi.org/10.1017/jfm.2013.509.

Tailleux, R., 2016a. Generalized patched potential density and thermodynamic neutral density: Two new physically based quasi-neutral density variables for ocean water masses analyses and circulation studies. J. Phys. Oceanogr. 46, 3571–3584. http://dx.doi.org/10.1175/JPO-D-16-0072.1.

Tailleux, R., 2016b. Neutrality versus materiality: a thermodynamic theory of neutral surfaces. Fluids 1, http://dx.doi.org/10.3390/fluids1040032.

Tailleux, R., 2018. Local available energetics of multicomponent compressible stratified fluids. J. Fluid Mech. 842, http://dx.doi.org/10.1017/jfm.2018.196.

Tailleux, R., 2021. Spiciness theory revisited, with new views on neutral density, orthogonality and passiveness. Ocean. Sci. 17, 203–219. http://dx.doi.org/10.5194/os-17-203-2021.

Tailleux, R., 2024. Negative available potential energy dissipation as the fundamental criterion for double diffusive instabilities. J. Fluid Mech. 994, http://dx.doi.org/10.1017/jfm.2024.647.

Tailleux, R., 2025. Is the Lorenz reference state global or local and observable? EGUsphere 2025, 1–7. http://dx.doi.org/10.5194/egusphere-2025-4595, URL: https://egusphere.copernicus.org/preprints/2025/egusphere-2025-4595/.

Tailleux, R., Dubos, T., 2024. A simple and transparent method for improving the energetics and thermodynamics of seawater approximations: Static energy asymptotics (SEA). Ocean. Model. 188, http://dx.doi.org/10.1016/j.ocemod.2024.102339.

Tailleux, R., Roullet, G., 2025. Energetically consistent localised ape budgets for local and regional studies of stratified flow energetics. Ocean. Model. 197, 102579. http://dx.doi.org/10.1016/j.ocemod.2025.102579, URL: https://www.sciencedirect.com/science/article/pii/S1463500325000824.

Tailleux, R., Wolf, G., 2023. On the links between thermobaricity, available potential energy, neutral directions, buoyancy forces, potential vorticity, and lateral stirring in the ocean. http://dx.doi.org/10.48550/arXiv.2202.00456, unpublished, available on https://arxiv.org/abs/2202.00456.

Torres, R., Waldman, R., Mak, J., Séférian, R., 2023. Global estimation of the eddy kinetic energy dissipation from a diagnostic energy balance. Geophis. Res. Lett. 50.

Veronis, G., 1975. The Role of Models in Tracer Studies. Numerical models of Ocean Circulation National Academy of Science, pp. 133–146.

Winters, K.B., Lombard, P.N., Riley, J.J., d'Asaro, E.A., 1995. Available potential energy and mixing in density stratified fluids. J. Fluid Mech. 289, 115–128.

Young, W.R., 2010. Dynamic enthalpy, conservative temperature, and the seawater boussinesq approximation. J. Phys. Oceanogr. 40, 394–400.

Young, W.R., 2012. An exact thickness-weighted average formulation of the Boussinesq equations. J. Phys. Oceanogr. 692–707.

Zemskova, V.E., White, B.L., Scotti, A., 2015. Available potential energy and the general circulation: partitioning wind, buoyancy forcing, and diapycnal mixing. J. Phys. Oceanogr. 45, 1510–1531.

Zilitinkevich, S.S., Elperin, T., Kleeorin, N., Rogachevskii, I., Esau, I., 2013. A hierarchy of energy- and flux (efb) turbulence closure models for stably-stratified geophysical flows. Boundary-Layer Meteorol 146, 341–373.